

Nitrous oxide and methane exchange in two small temperate forest catchments—effects of hydrological gradients and implications for global warming potentials of forest soils

Jesper Riis Christiansen · Lars Vesterdal ·
Per Gundersen

Received: 26 March 2010 / Accepted: 28 November 2010 / Published online: 14 December 2010
© Springer Science+Business Media B.V. 2010

Abstract The magnitude of greenhouse gas (GHG) flux rates may be important in wet and intermediate wet forest soils, but published estimates are scarce. We studied the surface exchange of methane (CH_4) and nitrous oxide (N_2O) from soil along toposequences in two temperate deciduous forest catchments: Strødam and Vestskoven. The soil water regime ranged from fully saturated to aerated within the catchments. At Strødam the largest mean flux rates of N_2O ($15 \mu\text{g N}_2\text{O-N m}^{-2} \text{ h}^{-1}$) were measured at volumetric soil water contents (SWC) between 40 and 60% and associated with low soil pH compared to smaller mean flux rates of $0\text{--}5 \mu\text{g N}_2\text{O-N m}^{-2} \text{ h}^{-1}$ for drier ($\text{SWC} < 40\%$) and wet conditions ($\text{SWC} > 80\%$). At Vestskoven the same response of N_2O to soil water content was observed. Average CH_4 flux rates were highly variable along the toposequences (-17 to $536 \mu\text{g CH}_4\text{-C m}^{-2} \text{ h}^{-1}$) but emissions were only observed above soil water content of 45%. Scaled flux rates of both GHGs to catchment level resulted in emission of 322 and 211 kg CO_2 -equivalents $\text{ha}^{-1} \text{ year}^{-1}$ for Strødam and Vestskoven, respectively, with N_2O contributing the most at both sites. Although the wet and intermediate wet forest soils occupied less than half the catchment area at both sites, the global warming potential (GWP) derived

from N_2O and CH_4 was more than doubled when accounting for these wet areas in the catchments. The results stress the importance of wet soils in assessments of forest soil global warming potentials, as even small proportions of wet soils contributes substantially to the emissions of N_2O and CH_4 .

Keywords Drainage · Forest soil · Methane · Nitrous oxide · Scaling · Wet soils

Introduction

The strong greenhouse gasses methane (CH_4) and nitrous oxide (N_2O) currently contribute about a fourth of the radiative forcing of the atmosphere caused by greenhouse gasses (Forster et al. 2007). Because the global warming potential of CH_4 and N_2O are 25 and 298 times stronger than CO_2 (in a 100 year time span), respectively, changes in the atmospheric concentration of these gasses are important in terms of global warming.

Forest soils (30% of the global land cover) are generally viewed as net sinks of CH_4 and sources of N_2O , but the exchange varies widely among forests (Pilegaard et al. 2006; Smith et al. 2000). Changes in the forest land use thus have the potential to alter the dynamics of N_2O and CH_4 .

Nitrous oxide and CH_4 production and consumption are the result of microbial processes occurring in soils, and the environmental controls on the flux

J. R. Christiansen (✉) · L. Vesterdal · P. Gundersen
Forest & Landscape Denmark, University of Copenhagen,
Rolighedsvej 23, 1958 Frederiksberg, Denmark
e-mail: jrc@life.ku.dk

dynamics of these gasses are related to oxygen, water and availability of mineral nitrogen (NH_4^+ and NO_3^-) and carbon sources. Nitrous oxide is formed in numerous, parallel processes in the soil; the most important of these processes being the denitrification and the nitrification of ammonium, as conceptualised in the hole-in-the-pipe model (Firestone and Davidson 1989). In laboratory and field studies, production of N_2O has been tightly coupled to water dynamics of the soil, with lowest flux rates at low as well as high water contents and highest flux rates at intermediate values (Davidson et al. 2000). Methane is consumed and produced in the soil by methanotrophs or methanogens, respectively, and soils can exhibit a highly dynamic pattern in terms of CH_4 flux rates with a net uptake changing to net emission of CH_4 if the soil becomes submerged (McNamara et al. 2006). Thus, the dynamics of both N_2O and CH_4 exchange in soils are related to changes in the environmental conditions with water as a key factor.

In recent decades, forest practice schemes directed towards “close-to-nature” management (Stanturf and Madsen 2002) has become more widespread in Europe and in many cases includes a reversion to natural hydrological conditions by ceased maintenance of ditches and drainage pipes. Inhibited soil drainage eventually leads to wetter conditions in forest soils and to the formation of intermediate or permanently wet soils. Thus, changed forest management and afforestation can lead to an increase in the proportion of wet forest soils and possibly affect the C and N cycle with consequences for the dynamics of GHGs.

In addition to soil moisture, soil pH and C/N ratio as well as the soil organic carbon (SOC) content have been proposed as important parameters to describe the magnitude and spatial distribution of GHG flux rates (Yamulki et al. 1997; Pilegaard et al. 2006). It is well known that aeration of a former anoxic soil matrix facilitates an oxidation of ferrous minerals and decomposition of organic matter releasing acids that can give rise to acidification and lower soil pH. Rewetting of the soil on the other hand inhibits oxidation and proton consuming processes act to stabilise or increase soil pH in a relatively short time (Szilas et al. 1998). Furthermore, low soil pH is often associated with high N_2O emissions and is recognised as an important parameter in regard to GHG dynamics (Weslien et al. 2009).

Drainage of soils has been proposed as a mitigation measure to reduce CH_4 emissions from wet soils (Dalal and Allen 2008), however von Arnold et al. (2005a, b) showed that while drainage of organic deciduous and coniferous forest soils decreased CH_4 emissions, CO_2 and N_2O emissions increased resulting in higher global warming potential compared to a non-drained site.

To improve emission estimates of global warming potentials from forest soils it is necessary to include a range of soil and hydrological conditions in order to scale GHG flux rates from point sources to landscape scale due to the dynamic nature of gaseous emissions from soils (Corre et al. 1999; Izaurralde et al. 2004; Jungkunst et al. 2004; Fiedler et al. 2005). However, small scale variability in soil properties can strongly influence the magnitude of flux rates (Weslien et al. 2009; Jungkunst et al. 2004; Jungkunst and Fiedler 2005).

The objectives of this study were to: (1) measure the surface exchange of CH_4 and N_2O in variable soil and hydrological conditions along toposequences in an old-growth beech forest (Strødam) and a young oak forest planted on former arable soil (Vestskoven) (2) to provide emission estimates for the whole study site by scaling chamber flux rates to catchment level using empirical models, (3) to quantify the importance of wet forest soils in relation to emission of N_2O and CH_4 and (4) to assess how a changing groundwater table would affect the global warming potential of the soils.

Materials and methods

Study sites

Two forest sites in Denmark, Strødam and Vestskoven, with contrasting previous land use were included in this study (Table 1). The Strødam site ($55^\circ 57' 25''$ N $12^\circ 16' 12''$ E) is a forest reserve established in 1949 with trees aged up to 250 years and has not been thinned or influenced by management practices since 1945. Historical maps document that this area has been forested for at least the last 160 years (National Survey and Cadastre 2009) and most likely for a longer period. The forest area is dominated by European beech, *Fagus sylvatica* L. The landscape is characterised as hummocky moraine and the soils

Table 1 Site and mineral soil characteristics from the two study sites

Location	Former land use	Tree species	Age (y)	P ^a T ^b N ^c _{dep}	Layer (cm)	Texture (weight%) (clay, silt, sand)	BD (g cm ⁻³)	pH CaCl ₂	SOC (%)	C:N ratio
Strødam	Forest	<i>Fagus Sylvatica</i> L. <i>Quercus Robur</i>	~150	657 7.8 14.8	0–5	4.5, 8.5, 87	0.57 ± 0.04	4.5 ± 0.3	8.3 ± 0.8	16.3 ± 0.3
					5–15	4.5, 8.5, 87	0.83 ± 0.04	4.4 ± 0.3	4.6 ± 0.4	16.0 ± 0.5
					15–30	3.9, 7.2, 88.9	1.11 ± 0.1	4.7 ± 0.2	2.4 ± 0.5	16.2 ± 0.7
					30–50	3.6, 6.5, 89.9	n.d.	5.2 ± 0.2	1.4 ± 0.3	17.1 ± 0.9
Vestskoven	Arable Orchard	<i>Quercus Robur</i>	30	594 7.9 12.3	0–5	14.9, 15, 70.1	0.77 ± 0.1	5.6 ± 0.2	4.8 ± 0.3	12.5 ± 0.2
					15–30	14.9, 15, 70.1	1.16 ± 0.1	5.8 ± 0.2	3.2 ± 0.3	11.3 ± 0.1
					5–15	19.7, 15.2, 65.1	1.40 ± 0.04	6.3 ± 0.2	2.4 ± 0.3	11.2 ± 0.3
					30–50	23.9, 15.2, 60.9	n.d.	6.5 ± 0.2	2.4 ± 0.4	11.6 ± 0.6

Bulk density (BD), soil pH CaCl₂, Soil organic C (SOC) and C/N ratio are means (±standard error of the mean) for all chambers (i.e. across the toposequences) at the site

N.d. not determined

^a Bold text refers to annual precipitation in mm

^b Italic text refers to mean annual temperature in (°C)

^c Annual total dissolved N deposition (NO₃-N + NH₄-N) in kg ha⁻¹. Numbers from similar nearby sites Gundersen et al. (2009)

consist of sandy loamy glacial till with spatially heterogenous distributed gravel patches and inclusions of peat accumulation in landscape depressions. General soil conditions are presented in Table 1.

The Vestskoven site (55°42'14" N 12°21'40" E) consists of evenly aged oak, *Quercus robur* L., planted in 1974 between the rows of a former apple orchard (dated 1950) (Table 1). According to historical maps the soil had been agricultural land at least since 1842 (National Survey and Cadastre 2009) and during this period the soil was drained. After afforestation the drain systems have not been maintained. The soil at Vestskoven is of glacial origin with low variation in texture composition of the soils throughout the catchment (Table 1).

At both sites small ponds form during periods of high rainfall and/or low evaporation but usually dry out during the summer. The water level in the ponds varied much throughout the study period. The soils not influenced by periodic occurrence of the lake were termed upland soils. The remaining soils were termed intermediate wet or permanently wet.

The local catchments were delineated based on two 1 km² extracts of a digital elevation model (DEM) (BlomInfo A/S, Copenhagen, Denmark) and estimated to 0.5 and 1.4 ha at Strødam and Vestskoven, respectively. The spatial resolution of the digital elevation model was 2.56 m², equivalent to a pixel size of 1.6 × 1.6 m, and the vertical resolution 0.1 m. At Vestskoven the northern border of the catchment was manually delineated to represent the maximum elevation studied at the site. Within the catchment at Strødam the elevation varied between 19.7 and 25.8 m (Fig. 1a). At Vestskoven the elevation range was 15.3–20.3 m (Fig. 1b).

Field design

The experimental design was similar for the two sites: Three transects were established and six to seven static chambers for gas exchange measurements were permanently installed along each transect (Fig. 1). Soil water content in 0–5 cm was measured at each chamber in all transects with a Theta probe ML2x (Delta T Devices, UK). Soil water content in 0–50 cm was measured in two of the three transects at both sites by time domain reflectometry using an electronic cable tester, 1502C Cable Tester (Tektronix, USA). Soil temperature was measured with a handheld

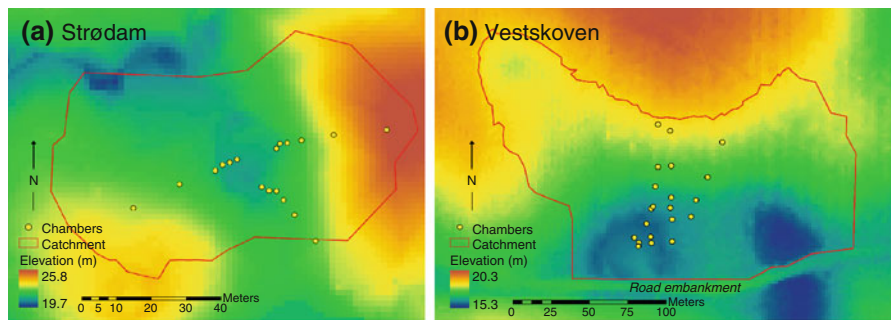


Fig. 1 Maps of the two study sites **a** Strødam and **b** Vestskoven. At both sites three transects were laid out with six to seven chambers for greenhouse gas measurements (dots).

A local catchment area was defined (line). At Vestskoven the catchment was confined on the southern perimeter by a road embankment

thermometer (model 550B, UEi, Beaverton, Oregon, USA). Groundwater depth (GWD) was recorded using perforated piezometers allowing water to infiltrate at ambient pressure. Three piezometers were installed along each transect. Measurements were conducted on a biweekly basis from May 2007 to August 2009 at Strødam and from May 2007 to October 2008 at Vestskoven. The position of each chamber was registered with GPS and transferred to the digital elevation model. The digital elevation model was used to estimate the elevation above sea level for each transect point by reading the elevation value for the cell located at the chamber position (Fig. 1).

Soil conditions along the transects

Intact cores of mineral soil (0–30 cm) were sampled at two points next to each chamber using an auger with an internal diameter of 5 cm (Westman 1995). Bulk density of the mineral soil fraction <2 mm cores were determined for three depth segments: 0–5, 5–15, and 15–30 cm. Intact cores were weighed and sieved (<2 mm) to remove stones and gravel. Roots were removed manually. The sieved samples were dried at 55°C to avoid volatilization of organic matter and were subsequently weighed. Subsamples were dried at 105°C for correction of weight. In some cases the volumetric fraction of stones exceeded 20% but was mostly in the range of 0–4%. Following determination of bulk density the two soil cores per chamber were pooled to one composite sample per depth segment. Mineral soil from 30 to 50 cm was sampled using an open-sided soil auger. A subsample of mineral soil samples was finally ground in an agate mortar for chemical analysis.

Ground samples of mineral soil were analysed for total C and N by dry combustion (Dumas method) in a Leco CSN 2000 Analyzer (Leco Corporation, St. Joseph, Michigan, USA). Mineral SOC for the fraction ≥ 2 mm was not assessed. No inorganic C (CaCO_3) was found within a 100 cm depth in soils at the two sites and all measured C were consequently considered to be of organic origin.

Mineral soil pH was measured on a Radiometer VIT 90 Video Titrator using a Radiometer GK2401 combination electrode (Radiometer, Denmark). Twelve grams of dried, sieved (<2 mm) and ground soil were mixed with 30 ml 0.01 M CaCl_2 solution and shaken for 2 h before measurement of pH.

Greenhouse gas exchange

Field measurements of gas exchange

The net soil surface exchange of CH_4 and N_2O was measured with closed static chambers. The chamber collar (inner diameter of 30.5 cm) was inserted 5 cm in the soil. Chamber headspace volumes ranged from 3.7 to 5.1 l. At measurement a lid was placed on top of the collar and sealed with a silicon rubber ring wrapped around the edge of the lid. Chamber headspace samples were taken with 60 ml plastic syringes through a butyl rubber septum in the middle of the lid at times 0, 30, 60 and 120 min. In March 2009 the enclosure time was reduced to 60 min and samples were taken every 20th min. The syringe was used to mix the headspace by pumping three times before fully filling the syringe. Samples were transferred to non-evacuated 2.7 ml crimped vials with a butyl rubber septum by flushing the vial with 58 ml

and pressurising the vial with the remaining 2 ml in the syringe.

Gas chromatography and calculation of gas flux rates

Gas samples were analysed on a Shimadzu GC-2014 gas chromatograph (Shimadzu, Kyoto, Japan) equipped with electron capture and flame ionisation detectors set at 300 and 200°C, respectively. The carrier gas was 100% N₂ with a flow rate of 25 ml min⁻¹. Methane and N₂O were analysed in separate columns set in a constant oven temperature of 40°C. The column used for CH₄ was a 60/80 Carboxen 1000 (15 ft, 1/8 in). For N₂O an 80/100 Hayesep Q (2.5 m, 1/8 in) column was used.

All gas flux rates were calculated by linear regression and expressed as µg N₂O-N m⁻² h⁻¹ or µg CH₄-C m⁻² h⁻¹. Linear regression analyses of the measurement series resulting in an *R*² value above 0.85 were accepted for flux rate calculation.

Scaling of greenhouse gas flux rates and drainage scenarios

Scaling of greenhouse gas flux rates

We used the Geographical Information System (GIS) software ArcMap 9.3.1 (ESRI, Redlands, CA, USA) to scale chamber N₂O and CH₄ flux rates to catchment level using the detailed digital elevation model. The GIS was also used to assess how changed drainage of the soil affected the magnitude of N₂O and CH₄ flux rates.

A relationship between annual mean soil water content and elevation for Strødam and between groundwater depth and elevation for Vestskoven was used to scale point measurements of hydrology to catchment level thus creating maps of soil water content in 0–5 cm and groundwater depth. The GHG flux rates were scaled by assigning the empirical response functions for GHG to the maps of soil water content and groundwater depth. The empirically modelled pixel values at the positions of the chambers were subsequently compared with the measured hydrology parameters and GHG flux rates for the chambers. In the following text modelled values refer to results obtained through the GIS analysis.

Drainage scenarios

The effect of raising or lowering the groundwater table was assessed by comparison of three scenarios: (i) restored natural hydrology (i.e. ditches and drainage pipes blocked) was represented as a fixed rise of the groundwater table of 50 cm (“+50 cm GWD”), (ii) improved soil drainage represented by maintaining a groundwater depth of >50 cm throughout the catchment (“–50 cm GWD”) and (iii) further improvement of the drainage system represented as a groundwater depth of >100 cm (“–100 cm GWD”).

For Vestskoven the “+50 cm GWD” scenario was not addressed because it would imply an extrapolation of N₂O and CH₄ flux rates beyond the range of the regression between groundwater depth and GHG flux rates resulting in unrealistically high flux rates of both N₂O and CH₄.

Statistics and data analysis

We investigated the influence of soil and hydrological characteristics along the toposequences using a backward stepwise regression analysis for each site (Sigmaplot 11.0, Systat Software Inc., Chicago, USA). Log-natural transformed mean flux rates of N₂O and CH₄ from all chambers at each site were related to the following parameters: SWC (0–5 cm), soil pH (0–5 cm), SOC (0–5 cm), bulk density (0–5 cm), C/N ratio (0–5 cm) and groundwater depth. Regression response functions for GHG flux rates were derived according to the results of the stepwise regression.

Greenhouse gas flux rates and soil water content measurements were paired in intervals corresponding to 5% vol for Strødam. The dataset consisting of mean N₂O and CH₄ flux rates and mean soil water content in 5 vol% intervals were used to establish response functions for the GHG exchange that are unbiased of the variable amount of observations over the whole range of soil water content. Linear regression analysis was performed using SAS 9.2 (SAS Institute Inc., Cary, USA, 2008) for response functions between soil water content and CH₄ (Strødam) and N₂O/CH₄ and groundwater depth (Vestskoven). Log-natural transformation was used when appropriate to ensure variance homogeneity. The non-linear regression procedure in SAS 9.2 was used to fit a bell-shaped response function between mean N₂O and mean soil

water content (Strødam). Predictions based on back-transformed log-natural regressions were corrected for bias by multiplying the predicted parameters with the Smearing Estimator (Duan 1983).

Significant differences between means of measured GHG flux rates at Strødam and Vestskoven for the same time period and N_2O flux rates for pH classes at Strødam were tested with simple *t*-test. Each pair of measured and empirically modelled values of soil water content, groundwater depth and GHG flux rates was subtracted and the mean of derivatives was tested for a significant difference from zero. A non-significant difference was interpreted as successful modelling. All the datasets subjected to statistical comparison were checked for normality (Shapiro–Wilk) and for normally distributed datasets a simple *t*-test was used. For non-normal distributed

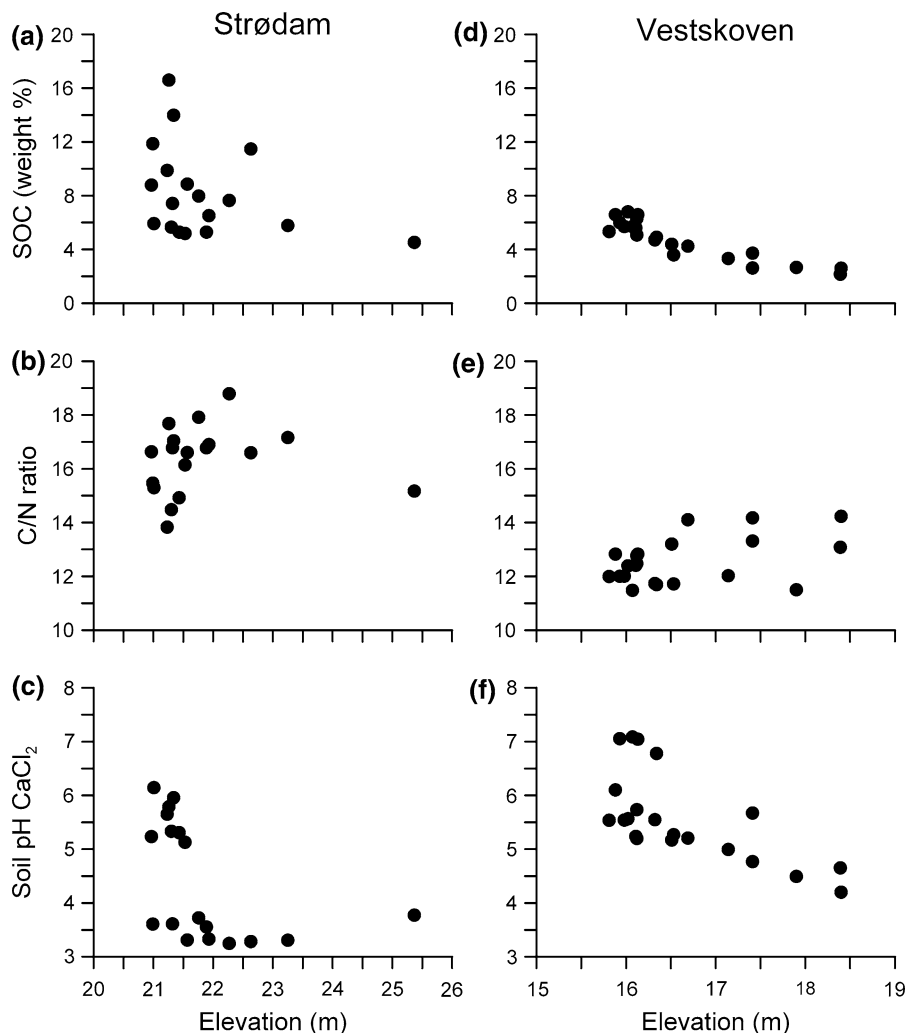
datasets the Mann–Whitney rank sum test was applied. For all statistical tests significance was accepted at the $p < 0.05$ level. Throughout the text mean values are accompanied when appropriate by \pm the standard error of the mean.

Results

Soil characteristics along the toposequences

At Strødam SOC content ranged from 18 to 4% (Fig. 2a), but there was no trend of SOC with elevation (Fig. 2a). At Vestskoven SOC displayed a consistent negative relationship with elevation decreasing from 5–6% at 16 m to 2% at 18.5 m (Fig. 2d). The variability was small probably as a

Fig. 2 Concentration of soil organic carbon (weight %) (SOC), C/N ratio and soil pH CaCl_2 for Strødam (a–c) and Vestskoven (d–f) in the top mineral soil (0–5 cm) vs. elevation above sea level in meters. Each circle represents a chamber in one of the three transects at each site



consequence of soil homogenisation from previous plowing and harrowing activities.

At Strødam the top mineral soil C/N ratio varied from 14 to 19 and was generally higher than at Vestskoven (11–14) (Fig. 2b and e), probably reflecting in part the legacy of fertilisation under arable land use in Vestskoven and partly the differences in soil types. At Strødam C/N ratios increased with elevation but similar to SOC there was a considerable variation for the lowest areas (Fig. 2b). At Vestskoven C/N ratios also increased with elevation, but varied considerably within the entire elevation range (Fig. 2e).

Soil pH displayed a consistent spatial pattern at Strødam where soil pH > 4 was only observed at elevations below 21.5 m. We attribute the higher soil pH in this region of the catchment to the presence of chronically wet soils. Only a few chambers below 21.5 m had soil pH < 4 and they were situated close to the 21.5 m contour line. The remaining chambers in the transects (above 21.5 m) had pH < 4 and showed no trend with elevation (Fig. 2c). Soil pH at Vestskoven decreased from 7 in the lowest parts to 4 in the highest parts (Fig. 2f).

Hydrological changes along the toposequences

The mean soil water content at Strødam in 0–5 cm showed a significant negative trend with elevation

(Fig. 3a, Table 2) and a similar trend was observed for soil water content in 0–50 cm. Accounting for bulk density along the transects the soil water regime ranged from fully saturated in the lowest parts of the transects to 30% WFPS in the highest parts for both the 0–5 cm and 0–50 cm layers. At Vestskoven there was no apparent trend in soil water content in the 0–5 cm layer with elevation but for 0–50 cm the soil water content decreased with elevation (Fig. 3c). Accounting for bulk density along the transect, the soil water regime in 0–50 cm ranged from around 80% WFPS in the lowest parts to 44% WFPS at the highest elevations.

The average groundwater depth clearly increased with elevation at both sites (Fig. 3b and d) and at Vestskoven the groundwater depth was significantly related to topography (Fig. 3d, Table 2).

Annual mean values of soil temperature (not shown) did not show any trend with elevation at both sites, and the mean soil temperature was regarded as constant along the transects.

N₂O flux rates

The flux rates of N₂O ranged from –20 to 150 µg N₂O-N m^{–2} h^{–1} at Strødam (Fig. 4a) and from –9 µg N₂O-N m^{–2} h^{–1} to 670 µg N₂O-N m^{–2} h^{–1}

Fig. 3 Mean volumetric soil water content (SWC) (vol%) in 0–5 cm (filled symbols) and 0–50 cm (open symbols) and groundwater depth (GWD) (cm) at Strødam (a–b) and Vestskoven (c–d). Error bars (±std error of the mean) represent the temporal variation. Trend lines and R^2 -values are shown for the relationship between SWC and GWD and elevation at Strødam and Vestskoven, respectively. Some error bars do not exceed the size of the symbols

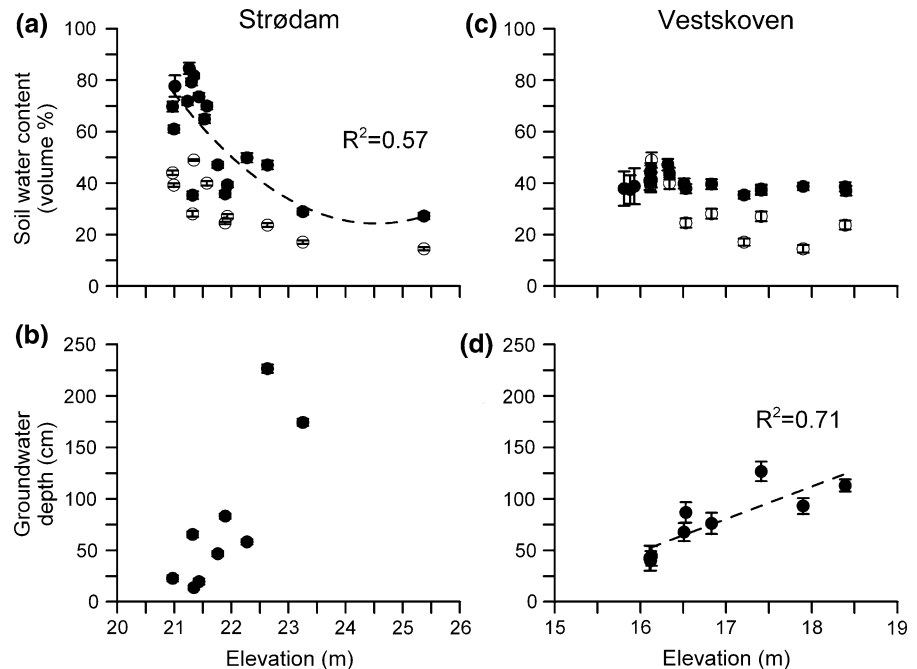
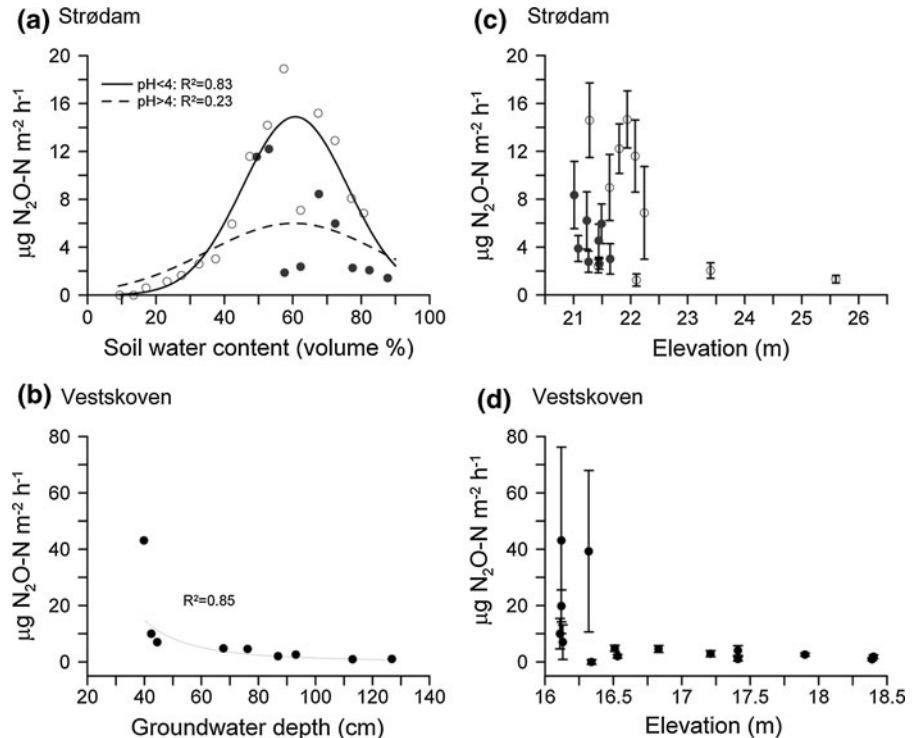


Table 2 Relationships between volumetric soil water content (SWC) in % and elevation (H) in meters and groundwater depth (GWD) and elevation (H) in meters for Strødam and Vestskoven, respectively

Site	Relationship	Equation	Statistics
Strødam	SWC _{0–5cm} (vol%) vs. elevation (m)	$SWC_{0–5cm}(H) = 2855 - 231.6 * H + 4.7 * H^2$ (1)	$R^2 = 0.58$ $p = 0.006$ $N = 18$
Vestskoven	GWD (cm) vs. elevation (m)	$GWD(H) = 31.5 * H - 455.9$ (2)	$R^2 = 0.71$ $p = 0.0044$ $N = 9$

Fig. 4 **a** Mean flux rates of N_2O ($\mu N_2O-N\ m^{-2}\ h^{-1}$) at Strødam related to mean volumetric soil water content (vol%) in the top mineral soil 0–5 cm for Strødam for soil pH > 4 (filled symbols) and soil pH < 4 (open symbols). **b** Mean flux rates of N_2O related to mean groundwater depth (cm) for Vestskoven. Trend lines and R^2 values are shown the relationship between hydrological properties and N_2O flux rates. Mean N_2O flux rates for each chamber related to elevation in meters at **c** Strødam for soil pH > 4 (filled symbols) and soil pH < 4 (open symbols) and **d** Vestskoven. Error bars (\pm std error of the mean) represent the temporal variation



at Vestskoven (Fig. 4b). At both sites the majority of N_2O flux rates were below $50\ \mu g\ N_2O-N\ m^{-2}\ h^{-1}$.

The N_2O flux exhibited a distinct pattern with lowest flux rates at both extremes of soil water content and an apparent maximum at intermediate water contents (60%, Fig. 4a), but non-significant or even negative flux rates were nevertheless still observed within this range in soil water content. The mean N_2O flux at Strødam ($6.4 \pm 0.5\ \mu g\ N_2O-N\ m^{-2}\ h^{-1}$) was lower but not significantly different from the mean N_2O flux at Vestskoven ($8.9 \pm 2.7\ \mu g\ N_2O-N\ m^{-2}\ h^{-1}$).

A soil pH of 4 was chosen as the value on which division of N_2O flux rates was based because of clear

shift in soil pH at low elevations (Fig. 2c). For chambers with soil pH < 4 N_2O flux rates ($7.6 \pm 0.8\ \mu g\ N_2O-N\ m^{-2}\ h^{-1}$) were significantly ($p = 0.045$) higher than N_2O flux rates ($4.2 \pm 0.5\ \mu g\ N_2O-N\ m^{-2}\ h^{-1}$) for chambers with pH > 4.

At both sites a topographic trend of N_2O flux rates was present (Fig. 4c and d). At Strødam the highest mean flux rates ($8\text{--}15\ \mu g\ N_2O-N\ m^{-2}\ h^{-1}$) were generally found at a height interval of 21.5 and 22.5 m, corresponding to a range in mean soil water content from 40 to 70 vol%. At elevations below 21.5 m N_2O flux rates were generally lower, but there was a considerable spatial variation (Fig. 4c). However, some of the spatial variation could be attributed

to soil pH as the low N_2O flux rates in this region represented chambers with soil $\text{pH} > 4$. At higher elevations in Strødam average N_2O flux rates were low ($< 2 \mu\text{g N}_2\text{O-N m}^{-2} \text{h}^{-1}$) (Fig. 4c). At Vestskoven the highest average N_2O flux rates were found below 16.5 m height, but there was a large both spatial and temporal variation (Fig. 4d). Above 16.5 m flux rates were consistently low ($< 5 \mu\text{g N}_2\text{O-N m}^{-2} \text{h}^{-1}$) showing no trend with elevation (Fig. 4d).

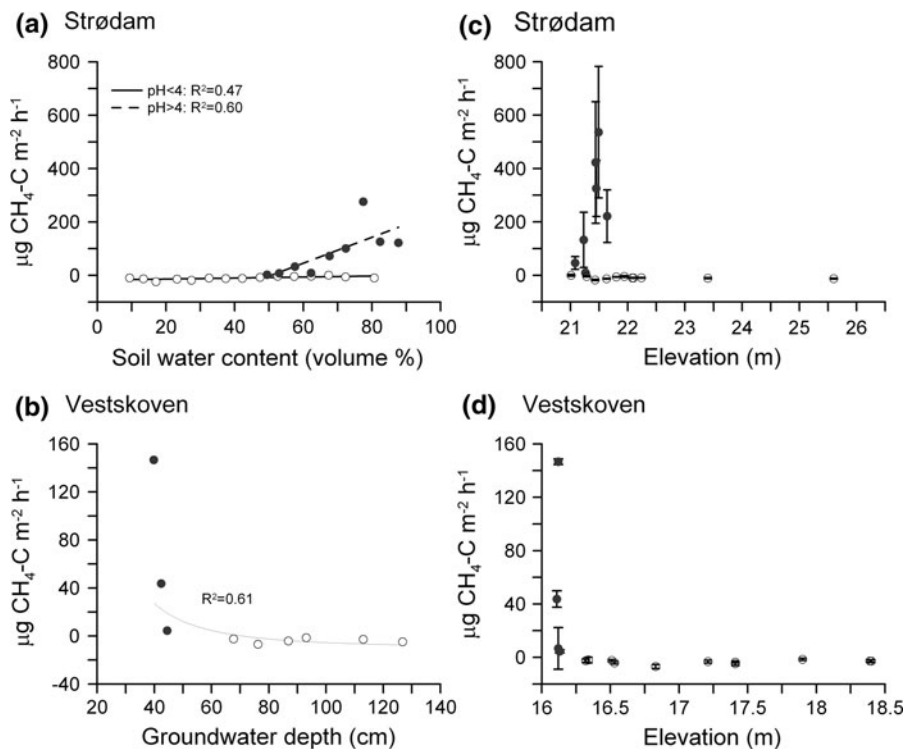
CH_4 flux rates

The CH_4 flux rates at both sites displayed a highly variable behaviour (Fig. 5a and b) and the CH_4 flux rates for Strødam ranged from -65 to $2200 \mu\text{g CH}_4\text{-C m}^{-2} \text{h}^{-1}$ (Fig. 5a). The CH_4 flux rates for Vestskoven ranged between -27 and $1600 \mu\text{g CH}_4\text{-C m}^{-2} \text{h}^{-1}$ (Fig. 5b). Emission of CH_4 was observed at soil water content above 45% (Fig. 5a and b) and the low-lying soils generally acted as net sources of CH_4 (Fig. 5c and d). Emission of CH_4 increased sharply with soil water content above this threshold at both sites (Fig. 5a and b). For chambers placed in the lowest parts of transects ebullition

events were observed but such events were excluded from the analysis due to the suspicion that the ebullition was caused by disturbance of the soil during sampling. Below a soil water content of 45% there was almost entirely uptake of CH_4 or non-significant flux rates at both sites (Fig. 5a and b), but CH_4 uptake occurred over the entire range of soil water content at Strødam (Fig. 5a). However, the upland soils primarily oxidised CH_4 (Fig. 5c and d). Emission of CH_4 also coincided with high soil pH which we attribute to the wet conditions in these soils.

The mean CH_4 flux including all data across the whole range of measured soil water content was significantly higher ($p < 0.0001$) at Strødam ($26 \pm 7.8 \mu\text{g CH}_4\text{-C m}^{-2} \text{h}^{-1}$) than the annual mean CH_4 at Vestskoven ($6.8 \pm 5.5 \mu\text{g CH}_4\text{-C m}^{-2} \text{h}^{-1}$). Dividing the CH_4 flux rates at a soil water content of 45% showed that the mean CH_4 flux for Strødam ($-10.4 \pm 0.7 \mu\text{g CH}_4\text{-C m}^{-2} \text{h}^{-1}$) was significantly ($p < 0.001$) smaller than the mean CH_4 flux at Vestskoven ($-1.1 \pm 1.6 \mu\text{g CH}_4\text{-C m}^{-2} \text{h}^{-1}$). However, at soil water content above 45% the mean CH_4 flux for Strødam ($59 \pm 14 \mu\text{g CH}_4\text{-C m}^{-2} \text{h}^{-1}$) was not significantly different than the mean CH_4 flux for Vestskoven ($80 \pm 53 \mu\text{g CH}_4\text{-C m}^{-2} \text{h}^{-1}$).

Fig. 5 **a** Mean flux rates of CH_4 ($\mu\text{g CH}_4\text{-C m}^{-2} \text{h}^{-1}$) at Strødam related to volumetric soil water content (%) in the top (0–5 cm) mineral soil for soil $\text{pH} > 4$ (filled symbols) and soil $\text{pH} < 4$ (open symbols). **b** Mean flux rates of CH_4 are related to mean groundwater depth (cm) for Vestskoven. Trend lines and R^2 values are shown the relationship between hydrological properties and CH_4 flux rates. Mean CH_4 flux rates for each chamber related to elevation at **c** Strødam and **d** Vestskoven. Error bars (\pm std error of the mean) represent the temporal variation. Open circles represent non-significant fluxes or uptake. Filled circles represent CH_4 emission



Response functions for N₂O and CH₄

The backward stepwise regression indicated that soil water content ($p = 0.003$) and soil pH ($p = 0.005$) at Strødam described the variation of observed N₂O flux rates. For CH₄ only soil water content in 0–5 cm was indicated ($p < 0.001$) as the best parameter to describe variations in CH₄ flux rates at Strødam. At Vestskoven groundwater depth ($p = 0.008$, $p = 0.032$) and bulk density ($p = 0.011$, $p = 0.002$) described best N₂O and CH₄ flux rates, respectively. An analysis showed that the inclusion of bulk density only had a minor influence on predicted N₂O and CH₄ flux rates compared to the results with groundwater depth alone and thus it was excluded in further calculations for Vestskoven.

Because there was a clear shift in soil hydrology and pH at an elevation of 21.5 m N₂O and CH₄ flux rates for Strødam were further divided in two groups above and below that height (Fig. 4a). The response functions for N₂O flux rates at Strødam had the form of a bell shaped curve with maximum flux rates at 60 vol% (Table 3). Equation 5 was not statistically significant but parameter values were identical to

those obtained by fitting an equation to individual measurement of N₂O and soil water content ($p < 0.0001$, not shown). Two linear functions between soil water content and CH₄ exchange was created with clear differences in their response to changes in soil water content (Table 3). Equation 4 represents the upland soils and Eq. 6 represents the intermediate to permanently wet soils (Table 3). At Vestskoven the functions for both gasses were based on the groundwater depth only and showed a strong curvilinear behaviour with altering groundwater depth (Table 3).

Scaling of hydrology and greenhouse gas flux rates to catchment level

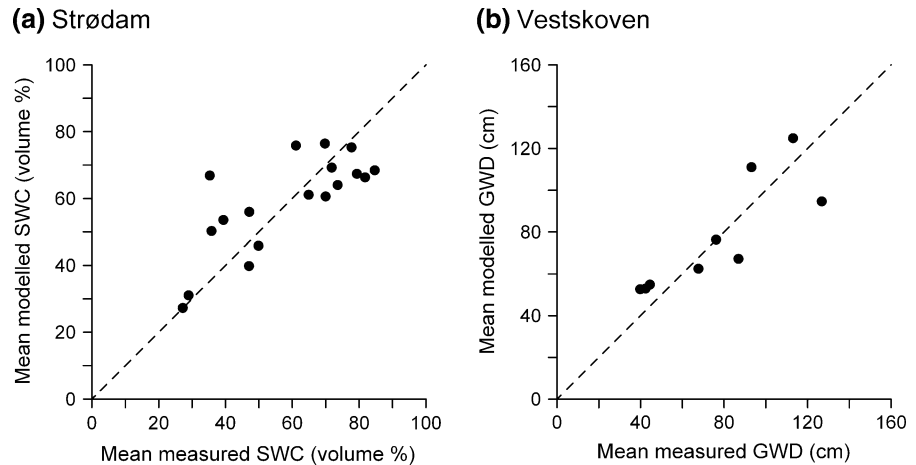
The empirical GIS model was able to predict the spatial variation in hydrological properties for Strødam and Vestskoven (Fig. 6a and b). At Strødam and Vestskoven the mean difference between measured and modelled values of soil water content ($p = 0.85$) and groundwater depth ($p = 0.90$), respectively, was not significantly different from zero.

Table 3 Response functions for N₂O and CH₄ at Strødam and Vestskoven based volumetric soil water content (SWC) in % and groundwater depth (GWD) in cm for Strødam and

Vestskoven, respectively. The units of the flux rates are $\mu\text{g N}_2\text{O-N m}^{-2} \text{ h}^{-1}$ and $\mu\text{g CH}_4\text{-C m}^{-2} \text{ h}^{-1}$

Site	Relationship	Equation	Statistics
Strødam soil pH < 4	N ₂ O vs. SWC	$f\text{N}_2\text{O} = \frac{14.9}{\text{Exp}\left(\frac{(\text{SWC}-60.7)^2}{2 \times 15.4^2}\right)}$ (3)	$R^2 = 0.83$ $p < 0.0001$ $N = 16$
	CH ₄ vs SWC	$f\text{CH}_4 = 0.18 * \text{SWC} - 17.8$ (4)	$R^2 = 0.47$ $p = 0.005$ $N = 15$
Strødam soil pH > 4	N ₂ O vs. SWC	$f\text{N}_2\text{O} = \frac{6.0}{\text{Exp}\left(\frac{(\text{SWC}-60.2)^2}{2 \times 25.2^2}\right)}$ (5)	$R^2 = 0.23$ $p = 0.07$ $N = 10$
	CH ₄ vs. SWC	$f\text{CH}_4 = 4.6 * \text{SWC} - 224$ (6)	$R^2 = 0.60$ $p = 0.009$ $N = 10$
Vestskoven	N ₂ O vs. GWD	$\text{Ln}(f\text{N}_2\text{O}) = -2.6 * \text{Ln}(\text{GWD}) + 12.3$ $f\text{N}_2\text{O} = 217549 * \text{GWD}^{-2.6}$ (7)	$R^2 = 0.85$ $p = 0.0004$ $N = 9$
	CH ₄ vs. GWD	$\text{Ln}(f\text{CH}_4 + 10) = -2.3 * \text{Ln}(\text{GWD}) + 12.1$ $f\text{CH}_4 = 179871 * \text{GWD}^{-2.3} - 10$ (8)	$R^2_{\text{adj}} = 0.61$ $p = 0.01$ $N = 9$

Fig. 6 Mean annual measured and modelled **a** volumetric soil water content (SWC) in % for Strødam and **b** groundwater depth (GWD) in cm for Vestskoven. The dashed line represents the 1:1 line. An empirical model applied in a geographic information system was used to model hydrological conditions at catchment level



The modelled N_2O flux at Strødam displayed a distinct spatial pattern with N_2O flux rates $<1.5 \mu\text{g N}_2\text{O-N m}^{-2} \text{ h}^{-1}$ in the lowest and highest parts of the catchment and highest flux rates ($6\text{--}16 \mu\text{g N}_2\text{O-N m}^{-2} \text{ h}^{-1}$) in an intermediate zone (Fig. 7a). The model was able to simulate the N_2O flux at Strødam within the variation of observed flux rates (Fig. 8a) and resulted in an emission of N_2O from the catchment of $0.88 \text{ kg N}_2\text{O ha}^{-1} \text{ year}^{-1}$ (Table 4). The mean difference between measured and modelled values of N_2O flux rates was not significantly ($p = 0.31$) different from zero.

The modelled CH_4 flux rates at Strødam ranged from -13 to $201 \mu\text{g CH}_4\text{-C m}^{-2} \text{ h}^{-1}$ (Fig. 7b) and resulted in an emission of CH_4 from the catchment of $2.4 \text{ kg CH}_4 \text{ ha}^{-1} \text{ year}^{-1}$ (Table 4). For a large part of the chambers a good agreement between observed and modelled uptake rates of CH_4 was obtained (Fig. 8b). However, the model estimated emission for three chambers even though field measurements indicated an annual mean uptake. In regard to CH_4 emission the model both under and overestimated the flux with no systematic trend (Fig. 8b). For two chambers the empirical model estimated CH_4 uptake even though there was an annual emission (Fig. 8b).

At Vestskoven modelled N_2O and CH_4 flux rates displayed the same spatial pattern, with highest flux rates in low-lying parts of the catchment (not shown). The modelled N_2O flux rates ranged from <1 to $43 \mu\text{g N}_2\text{O-N m}^{-2} \text{ h}^{-1}$ and for CH_4 flux rates ranged from $-9 \mu\text{g CH}_4\text{-C m}^{-2} \text{ h}^{-1}$ in the higher parts to $101 \mu\text{g CH}_4\text{-C m}^{-2} \text{ h}^{-1}$ in the low-lying parts

resulting in emission of both N_2O ($0.68 \text{ kg N}_2\text{O ha}^{-1} \text{ year}^{-1}$) and CH_4 ($0.37 \text{ kg CH}_4 \text{ ha}^{-1} \text{ year}^{-1}$) (Table 4). The relationship between modelled and measured flux rates of N_2O flux rates at Vestskoven was acceptable when flux rates ranged between 0 and $10 \mu\text{g N}_2\text{O-N m}^{-2} \text{ h}^{-1}$, as the mean difference between measured and modelled values was not significantly ($p = 0.54$) different from zero, but higher flux rates were underestimated by the GIS modelling (Fig. 8d).

The modelled CH_4 flux rates did not compare well with measured values, e.g. CH_4 emission was in most cases underestimated and observed CH_4 uptake was modelled as CH_4 emission in some cases (Fig. 8d). The modelled flux rates of CH_4 at both sites must be treated with caution due to the extreme spatial and temporal variation observed for measured CH_4 flux rates which complicate scaling of CH_4 flux rates to catchment level.

Drainage scenarios

At Strødam two criteria were assessed for the scenario analysis: (a) Soil pH changes were assumed to affect only N_2O and to account for expected changes in soil pH the critical groundwater depth was found where the soil pH threshold of 4 was met. Thus, it was possible to delineate the zones of different pH for each scenario and (b) soil water content in 0–5 cm and groundwater depth was related in order to apply the response functions for N_2O and CH_4 . At Strødam the critical groundwater depth where the threshold soil pH of 4 was met was

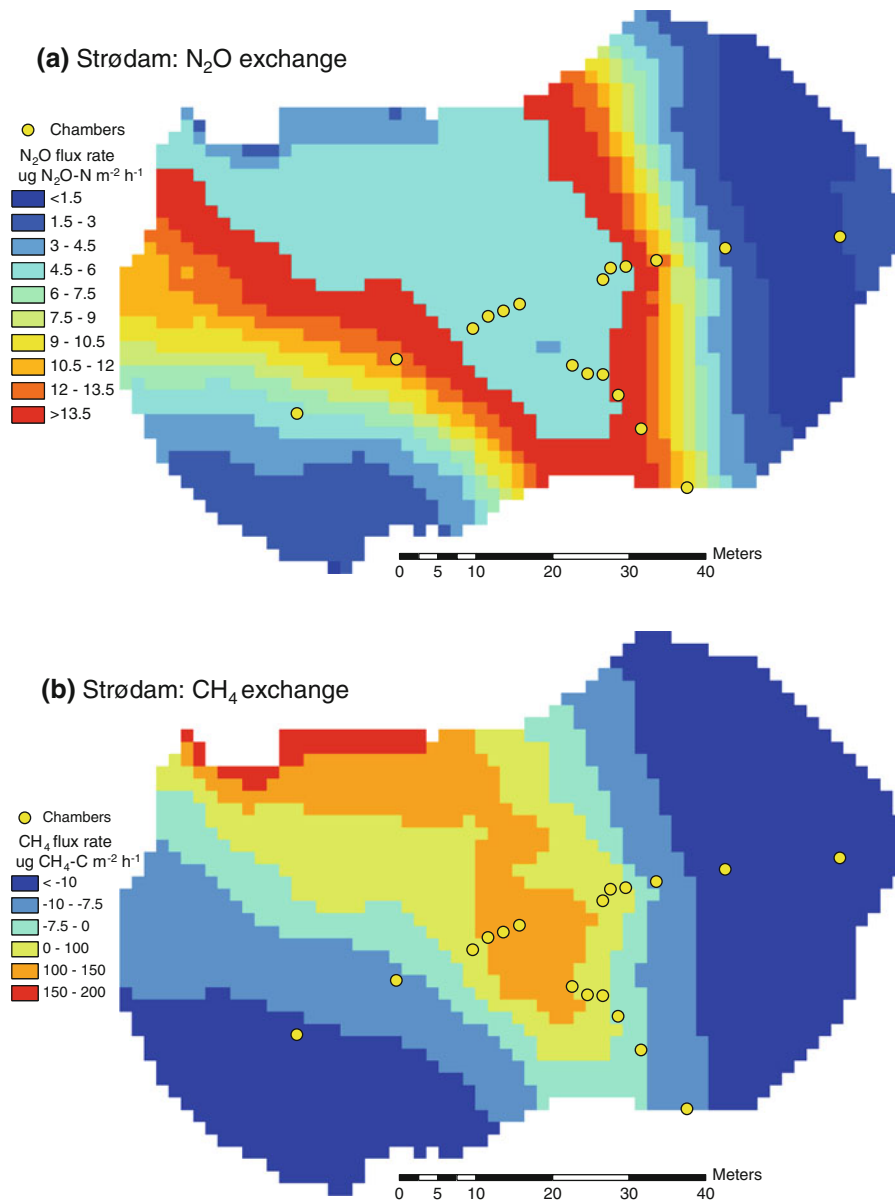


Fig. 7 Maps of modelled **a** N₂O exchange ($\mu\text{g N}_2\text{O-N m}^{-2} \text{ h}^{-1}$) and **b** CH₄ exchange ($\mu\text{g CH}_4\text{-C m}^{-2} \text{ h}^{-1}$) at Strødam. Greenhouse gas flux rate were modelled at catchment level

using a geographic information system. Chambers placed in three transects are represented by dots

estimated to be 50 cm. Thus, for “+50 cm GWD” an elevated groundwater table would result in a change of soil pH to values larger than 4 for a part of the catchment that previously had soil pH lower than 4 while for “−50 cm GWD” and “−100 cm GWD” it was assumed that soil pH would decrease below 4 for the whole catchment. All three drainage scenarios were evaluated at Strødam by use of the following

significant relationship between soil water content in 0–5 cm (Fig. 3a) and groundwater depth (Fig. 3b):

$$\text{SWC} = 200.3 * \text{GWD}^{-0.34}$$

$$(R^2 = 0.81, p < 0.0001, N = 9) \quad (9)$$

Compared to the present situation at Strødam N₂O emissions increased slightly from 262 to 280–281 kg CO₂e ha^{−1} year^{−1} for the “+50 cm GWD” and

Fig. 8 Comparison of mean measured and modelled **a** N_2O flux rates ($\mu\text{g N}_2\text{O-N m}^{-2} \text{h}^{-1}$) for Strødam, **b** CH_4 flux ($\mu\text{g CH}_4\text{-C m}^{-2} \text{h}^{-1}$) rates for Strødam, **c** N_2O flux rates for Vestskoven and **d** CH_4 flux rates for Vestskoven. Open circles represent measured uptake of CH_4 and filled circles represent measured emission of CH_4 . The dashed lines are 1:1 lines

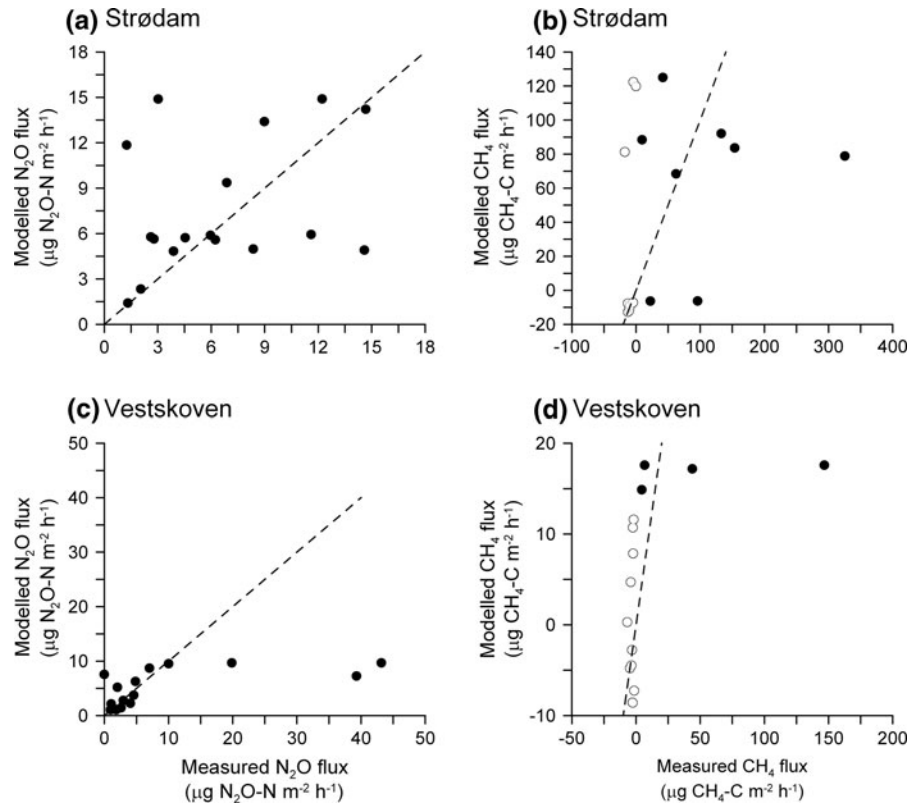


Table 4 Modelled annual mean flux rates and their sum converted to CO_2 -equivalents of N_2O and CH_4 for the catchments at Strødam and Vestskoven (in *italics*)

	Area ^a ha	N_2O	CH_4	CO_2 -equivalents		
		Modelled annual mean $\text{kg N}_2\text{O ha}^{-1} \text{year}^{-1}$	Modelled annual mean $\text{kg CH}_4 \text{ha}^{-1} \text{year}^{-1}$	$\text{N}_2\text{O kg CO}_2\text{e ha}^{-1} \text{year}^{-1}$	$\text{CH}_4 \text{kg CO}_2\text{e ha}^{-1} \text{year}^{-1}$	Sum $\text{kg CO}_2\text{e ha}^{-1} \text{year}^{-1}$
Strødam	0.5	0.88 (0.45–1.3)	2.4 (0.50–4.3)	262 (134–385)	60 (13–107)	322 (146–492)
Vestskoven	1.4	0.68 (0.40–1.2)	0.37 (–0.7–3.4)	203 (121–356)	8 (–15–71)	211 (106–427)

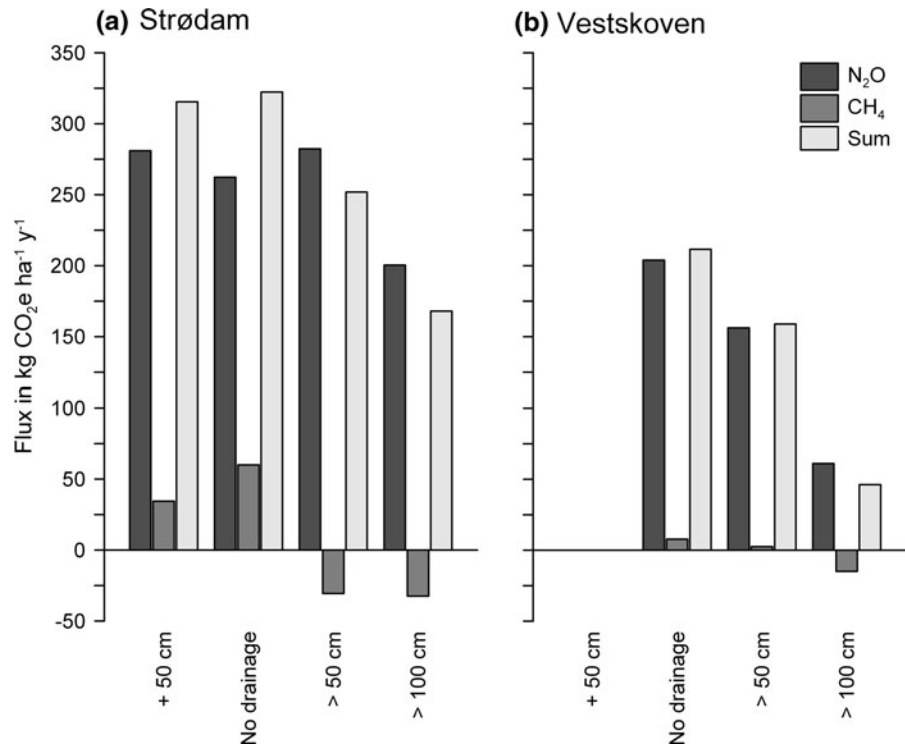
The 95% confidence-intervals of estimates are shown in brackets. Modelled annual mean flux was converted to CO_2 -equivalents by multiplying with a factor of 298 and 25 for N_2O and CH_4 , respectively (Forster et al. 2007)

^a The area of the local catchment

“–50 cm GWD” scenarios, respectively (Fig. 9a). However, N_2O emissions decreased to $200 \text{ kg CO}_2\text{e ha}^{-1} \text{year}^{-1}$ when draining further to a 100 cm (Fig. 9a). The soil was still a net source ($34 \text{ kg CO}_2\text{e ha}^{-1} \text{y}^{-1}$) of CH_4 in the “+50 cm GWD” scenario. However, for the “–50 cm GWD” and “–100 cm GWD” scenarios the soil was a net sink of CH_4 by 30 and $32 \text{ kg CO}_2\text{e ha}^{-1} \text{year}^{-1}$, respectively.

The total source strength in CO_2 -equivalents of N_2O and CH_4 was reduced by 2, 22 and 48% for the scenarios “+50 cm GWD”, “–50 cm GWD” and “–100 cm GWD”, respectively (Fig. 9a). For Vestskoven N_2O emissions decreased to $156 \text{ kg CO}_2\text{e ha}^{-1} \text{year}^{-1}$ for the “–50 cm GWD” scenario and decreased further to $61 \text{ kg CO}_2\text{e ha}^{-1} \text{year}^{-1}$ for the “–100 cm GWD” (Fig. 9b). The CH_4 emission decreased to $3 \text{ kg CO}_2\text{e ha}^{-1} \text{year}^{-1}$ for “–50 cm

Fig. 9 Total annual catchment emission of CO₂-equivalents (kg CO₂e ha⁻¹ y⁻¹) of N₂O, CH₄ and the CO₂-equivalent sum of the two gasses at **a** Strødam and **b** Vestskoven for the current situation (“No drainage”), a 50 cm raise of the groundwater level (“+50 cm GWD”), a 50 cm lowering of the groundwater level (“-50 cm GWD”) and a 100 cm lowering of the groundwater level (“-100 cm GWD”)



GWD” and the soil became a net sink of CH₄ of 15 kg CO₂e ha⁻¹ year⁻¹ for the “-100 cm GWD” scenario (Fig. 9b). The total source strength of the soil at Vestskoven decreased by 25 and 78% for the “-50 cm GWD” and “-100 cm GWD” scenarios, respectively.

Discussion

N₂O flux rates

The mean measured N₂O flux for our sites at 0.56 ± 1.1 and 0.78 ± 4.2 kg N₂O-N ha⁻¹ year⁻¹ for Strødam and Vestskoven, respectively, was in the same range as the mean N₂O flux of 0.45 ± 0.48 kg N₂O-N ha⁻¹ year⁻¹ for a beech (*Fagus sylvatica*) forest in Sorø, Denmark, with a similar climate and N deposition regime (Skiba et al. 2009) and for European temperate forests in general (N₂O: 0–1.8 kg N₂O-N ha⁻¹ year⁻¹, Pilegaard et al. (2006)).

The distribution of soil water content at the catchment scale was reported to control the activity of denitrifying bacteria in the soil and consequently

the surface flux (Florinsky et al. 2004). We also found that soil hydrology exerted the strongest control on the spatial distribution of N₂O flux rates (Fig. 4c and d). Furthermore, the measured and modelled maximum flux rates of N₂O peaked at intermediate soil water content as also reported in other studies (i.e. Davidson et al. 2000; Flechard et al. 2007).

Soil pH, besides soil water content, influenced N₂O emissions at Strødam as suggested by the significantly different N₂O flux rates of the classes for soil pH (Table 3). These findings concur with Weslien et al. (2009) who found high N₂O flux rates for soils with low pH. Soil pH directly affects the N₂O production in the soil by inhibiting the activity of the nitrous oxide reductase enzyme at low pH thus increasing N₂O emissions (Firestone and Davidson 1989). Therefore, the distribution of soil pH within the catchment as observed at Strødam was an additional factor explaining the spatial distribution of N₂O flux rates. At Vestskoven where low soil pH was confined to the dry end of the transects no influence of pH could be detected.

Our measurements of N₂O flux rates, soil pH and hydrology point to the importance of evaluating the interaction between hydrology and soil conditions to

understand the spatial variation of N_2O flux rates. Thus, the hydrological regime interacted with the soil to create different zones of soil pH, probably due to buffering from periodic rise of groundwater at elevations <21.5 m that in turn controlled the production of N_2O in the soil.

CH_4 flux rates

The measured mean annual emission of CH_4 at Strødam and Vestskoven (2.4 ± 0.7 and 0.59 ± 8.6 kg $\text{CH}_4\text{-C ha}^{-1} \text{ year}^{-1}$, respectively) was larger compared to a net CH_4 uptake for the well-drained Sorø beech forest (-3.9 ± 1.7 kg $\text{CH}_4\text{-C ha}^{-1} \text{ year}^{-1}$) (Skiba et al. 2009) and a range of European forests (CH_4 : -2.3 to -10 kg $\text{CH}_4\text{-C ha}^{-1} \text{ year}^{-1}$ (Skiba et al. 2009)). At our sites the presence of waterlogged soils was responsible for the net emission, showing that inclusion of wet forest soils are important in order to assess whether the soil is a source or a sink of CH_4 , as it has otherwise been reported for European forest soils (Ball et al. 1997; Smith et al. 2000).

Along the transects at the two sites both net annual uptake and net annual emission of CH_4 was observed reflecting the complex nature of CH_4 flux rates. At both sites CH_4 uptake increased with decreasing soil water content which is consistent with recent findings (i.e. Guckland et al. 2009). Similar to McNamara et al. (2006) we found that net annual CH_4 emission occurred at a shallow groundwater table and a net uptake was observed for the same soils once the groundwater table was lowered. Thus, soil hydrology controlled the direction and magnitude of CH_4 flux rates at our study sites and explained the observed spatial pattern (Fig. 5c and d).

The significantly higher uptake rate of CH_4 at Strødam than at Vestskoven in the dry end of transects ($\text{SWC} < 45\%$) was caused by differences in land use history and soil structure. It is likely that a slow recovery of the CH_4 oxidising microbial community after afforestation of this former agricultural soil as shown by Priemé et al. (1997) was responsible for the lower CH_4 uptake at Vestskoven. Also, the higher bulk density and finer texture of the soil at Vestskoven compared to Strødam would reduce CH_4 uptake rates (Ball et al. 1997; Boeckx et al. 1997).

The non-significantly different CH_4 flux rates above soil water content of 45% between the two sites was attributed to the huge variability observed

for CH_4 emissions (Fig. 5a and b). For all wet soils at both sites ebullition of CH_4 was observed and it can not be excluded that the high observed emissions of CH_4 were partly caused by ebullition during measurement causing episodic high emissions although obvious cases were excluded. Ebullition of CH_4 is a spatially and temporally highly variable phenomenon and has been proposed as the dominant transport mechanism for CH_4 in peat soils (Waddington et al. 2009).

Overall, the distribution of wet and upland areas explain the spatial variation of the CH_4 flux rates but the magnitude of CH_4 uptake are related to site specific land use history and soil types.

Scaling of hydrology and greenhouse gas flux rates

The chambers were located in such a manner that they represented most of the conditions found within the catchment and the empirical modelling of hydrology at Strødam and Vestskoven was able to simulate the spatial variation of these properties (Fig. 6a and b).

Contrary to the measurements of N_2O flux rates, the modelled catchment emission of N_2O was slightly lower at Vestskoven than at Strødam, but the magnitude of modelled and measured N_2O flux rates was comparable (Table 4). A part of the catchment at Vestskoven with low modelled N_2O flux rates extended farther beyond the transects than what was the case at Strødam. Consequently, the catchment mean at Vestskoven would be lower by including these areas than what was indicated by the measurements.

The scaled catchment flux rates of CH_4 (Table 4) must be treated with caution as the modelled CH_4 emissions were greatly underestimated. However, the method of calculating CH_4 flux rates based on response functions for wet and upland soils (Strødam) tend to work better than aiming at calculating CH_4 flux rates using one equation that encompasses all hydrological conditions as for Vestskoven. Still, a better description of the response of CH_4 flux rates to hydrology, especially near saturation and at fully saturated conditions, is needed in order to improve the catchment emission estimate of CH_4 . However, in line with measurements of CH_4 , a net emission of CH_4 was modelled at both Strødam and Vestskoven.

Importance of wet forest soils for greenhouse gas emissions

Assuming that upland soils at maximum could attain an annual mean soil water content of 50% at Strødam, modelled N_2O and CH_4 flux rates would amount to $0.60 \text{ kg N}_2\text{O ha}^{-1} \text{ year}^{-1}$ and $-1.3 \text{ kg CH}_4 \text{ ha}^{-1} \text{ year}^{-1}$, equivalent to a total of $147 \text{ kg CO}_2\text{e ha}^{-1} \text{ year}^{-1}$. At Vestskoven the catchment CO_2e emission ($\text{N}_2\text{O} + \text{CH}_4$) from upland soils, defined as soils with a mean groundwater table deeper than 50 cm, would be $94 \text{ kg CO}_2\text{e ha}^{-1} \text{ year}^{-1}$. Considering the estimated actual CO_2e emissions of 322 and $213 \text{ kg CO}_2\text{e ha}^{-1} \text{ year}^{-1}$ at Strødam and Vestskoven, respectively (Table 4), it can be concluded that accounting for the wet soils more than double the estimated catchment global warming potential even though they constitute less than half of the area within the catchments at Strødam and Vestskoven. A similar conclusion was reached by Jungkunst and Fiedler (2005), who found that by including all soil types, also wet soils, within a small forest catchment the emission of CO_2e increased from $355 \text{ kg CO}_2\text{e ha}^{-1} \text{ year}^{-1}$ for upland soils to $1059 \text{ kg CO}_2\text{e ha}^{-1} \text{ year}^{-1}$. Our findings further emphasises the importance of including the intermediate to permanently wet forest soils in the assessment, as the global warming potential would otherwise have been underestimated.

Effect of altering groundwater table on global warming potential of the forest soil

Our scenario analysis of drainage suggested increased N_2O emission following improved drainage to 50 cm depth (Fig. 9a) as it was also reported for deciduous forests on organic soils (von Arnold et al. 2005a). It was suggested that drainage improved aeration in the soil thereby initiating decomposition of SOC and associated mineralisation of organic N that in turn stimulated N_2O production (Klemetsson et al. 2005; von Arnold et al. 2005a). In our case drainage could also imply an acidification of the lower parts of the catchment that would further favour N_2O production in the soil at Strødam. However, further drainage to 100 cm will imply, according to our relationships (Eqs. 3 and 5 in Table 3) that soil moisture becomes too low and in that case restricts N_2O production in the soil as a whole even though the availability of N

might be higher at $\text{pH} < 4$. Consistent with the findings of von Arnold et al. (2005a) improved drainage decreased CH_4 emission and even turned it into a net sink of CH_4 (for scenarios “−50 cm GWD” and “−100 cm GWD”). The marginal lower CH_4 emission for the “+50 cm GWD” scenario was caused by a smaller areal extent of the zone where CH_4 production would occur according to our findings.

Our results suggest that reduced soil drainage will increase the emission of CO_2 -equivalents derived from N_2O and CH_4 , mainly because the areal proportion of intermediate wet to wet soils will increase and thereby emit more N_2O , oxidise less CH_4 than upland soils and emit CH_4 . However, reduced drainage does not *per se* lead to increased global warming potential as we also estimated. The magnitude of change in global warming potential also depends on how the zones of GHG emission and uptake distribute at the landscape scale which is related to the geomorphology of the catchments (Jungkunst and Fiedler 2005).

In line with our study Yu et al. (2008) found that the global warming potential of submerged mineral soils (swamp) was higher than that of upland mineral soils (ridge). According to Schulze et al. (2010) C sequestration in forest soil and biomass for continental Europe was ~ 700 and $\sim 2000 \text{ kg CO}_2\text{e ha}^{-1} \text{ year}^{-1}$, respectively. With the estimated global warming potential from N_2O and CH_4 at our sites of $213\text{--}322 \text{ kg CO}_2\text{e ha}^{-1} \text{ year}^{-1}$ this is largely offset by C sequestration in biomass in managed forests and afforested sites, such as Vestskoven. However, at the old-growth forest, Strødam, the soil must be considered as the main sink for atmospheric C, meaning that the emission of N_2O and CH_4 may be only just be compensated by soil C sequestration. Furthermore, adding the importance of wet forest soils in relation to enhanced emission of strong greenhouse gasses future estimates of C sequestration in forested landscape must be downgraded.

Conclusion

This study showed that accounting for enhanced emissions of N_2O and CH_4 from intermediate wet and wet forest soils doubled the global warming potential from these gasses at the catchment level even though these soils comprised less than half of the catchment

area at the two study sites, Strødam and Vestskoven, respectively. Thus, we conclude that the emissions of N_2O and CH_4 from forests will increase by increasing the areal proportion of intermediate wet to wet forest soils and it is expected that the global warming potential, derived from N_2O and CH_4 , of forests soils will increase in the future as a consequence of changed land use, e.g. rewetting of previously drained soils, within the forests.

Acknowledgments We are grateful to Preben Frederiksen, Xhevat Haliti, Mads Krag and Yunting Fang for help in the field. This study was part of NitroEurope IP. The research was further supported financially by the RECETO PhD school and the Faculty of Life Sciences both at University of Copenhagen.

References

- Ball BC, Smith KA, Klemmedtsson L et al (1997) The influence of soil gas transport properties on methane oxidation in a selection of northern European soils. *J Geophys Res Atmos* 102:23309–23317
- Boeckx P, Van Cleemput O, Villaralvo I (1997) Methane oxidation in soils with different textures and land use. *Nutr Cycl Agroecosyst* 49:91–95
- Corre MD, Pennock DJ, Van Kessel C et al (1999) Estimation of annual nitrous oxide emissions from a transitional grassland-forest region in Saskatchewan, Canada. *Biogeochemistry* 44:29–49
- Dalal RC, Allen DE (2008) Greenhouse gas fluxes from natural ecosystems. *Aust J Bot* 56:369–407
- Davidson EA, Keller M, Erickson HE et al (2000) Testing a conceptual model of soil emissions of nitrous and nitric oxides. *Bioscience* 50:667–680
- Duan N (1983) Smearing estimate—a nonparametric retransformation method. *J Am Stat Assoc* 78:605–610
- Fiedler S, Holl BS, Jungkunst HF (2005) Methane budget of a Black Forest spruce ecosystem considering soil pattern. *Biogeochemistry* 76:1–20
- Firestone MK, Davidson EA (1989) Microbiological basis of NO and N_2O production and consumption in soil. In: Andreae MO, Schimel DS (eds) *Exchange of trace gases between terrestrial ecosystems, the atmosphere*. Wiley, Chichester, UK
- Flechard CR, Ambus P, Skiba U et al (2007) Effects of climate and management intensity on nitrous oxide emissions in grassland systems across Europe. *Agric Ecosyst Environ* 121:135–152
- Florinsky IV, McMahon S, Burton DL (2004) Topographic control of soil microbial activity: a case study of denitrifiers. *Geoderma* 119:33–53
- Forster P, Ramaswamy V, Artaxo P et al (2007) Changes in atmospheric constituents and in radiative forcing. In: Solomon S, Qin D, Manning M et al (eds) *Climate change 2007: the physical science basis. Contribution of working group I to the fourth assessment report of the intergovernmental panel on climate change*, Chapter 2. Cambridge University Press, Cambridge
- Guckland A, Flessa H, Prenzel J (2009) Controls of temporal and spatial variability of methane uptake in soils of a temperate deciduous forest with different abundance of European beech (*Fagus sylvatica* L.). *Soil Biol Biochem* 41:1659–1667
- Gundersen P, Sevel L, Christiansen JR et al (2009) Do indicators of nitrogen retention and leaching differ between coniferous and broadleaved forests in Denmark? *For Ecol Manag* 258:1137–1146
- Izaurrealde RC, Lemke RL, Goddard TW et al (2004) Nitrous oxide emissions from agricultural toposequences in Alberta and Saskatchewan. *Soil Sci Soc Am J* 68:1285–1294
- Jungkunst HF, Fiedler S (2005) Geomorphology—key regulator of net methane and nitrous oxide fluxes from the pedosphere. *Zeitschrift für Geomorphologie* 49:529–543
- Jungkunst HF, Fiedler S, Stahr K (2004) N_2O emissions of a mature Norway spruce (*Picea abies*) stand in the Black Forest (southwest Germany) as differentiated by the soil pattern. *J Geophys Res Atmos* 109:1–11
- Klemmedtsson L, Von Arnold K, Weslien P et al (2005) Soil CN ratio as a scalar parameter to predict nitrous oxide emissions. *Global Change Biol* 11:1142–1147
- McNamara NP, Chamberlain PM, Pearce TG et al (2006) Impact of water table depth on forest soil methane turnover in laboratory soil cores deduced from natural abundance and tracer C-13 stable isotope experiments. *Isot Environ Health Studies* 42:379–390
- National Survey and Cadastre (2009) <http://kmswww3.kms.dk/kortpaanettet/dkfoerognu.htm>. Accessed 1 Oct 2009
- Pilegaard K, Skiba U, Ambus P et al (2006) Factors controlling regional differences in forest soil emission of nitrogen oxides (NO and N_2O). *Biogeosciences* 3:651–661
- Priemé A, Christensen S, Dobbie KE, Smith KA (1997) Slow increase in rate of methane oxidation in soils with time following land use change from arable agriculture to woodland. *Soil Biol Biochem* 29:1269–1273
- Schulze ED, Clais P, Luyssaert S et al (2010) The European carbon balance. Part 4: integration of carbon and other trace-gas flux rates. *Global Change Biol* 16:1451–1469
- Skiba U, Drewer J, Tang YS et al (2009) Biosphere-atmosphere exchange of reactive nitrogen and greenhouse gases at the NitroEurope core flux measurement sites: measurement strategy and first data sets. *Agric Ecosyst Environ* 133:139–149
- Smith KA, Dobbie KE, Ball BC et al (2000) Oxidation of atmospheric methane in Northern European soils, comparison with other ecosystems, and uncertainties in the global terrestrial sink. *Global Change Biol* 6:791–803
- Stanturf JA, Madsen P (2002) Restoration concepts for temperate and boreal forests of North America and Western Europe. *Plant Biosyst* 136:143–158
- Szilas CP, Borggaard OK, Hansen HCB et al (1998) Potential iron and phosphate mobilization during flooding of soil material. *Water Air Soil Pollut* 106:97–109
- Von Arnold K, Nilsson M, Hanell B et al (2005a) Fluxes of CO_2 , CH_4 and N_2O from drained organic soils in deciduous forests. *Soil Biol Biochem* 37:1059–1071

- Von Arnold K, Weslien P, Nilsson M et al (2005b) Fluxes of CO₂, CH₄ and N₂O from drained coniferous forests on organic soils. *For Ecol Manag* 210:239–254
- Waddington JM, Harrison K, Kellner E et al (2009) Effect of atmospheric pressure and temperature on entrapped gas content in peat. *Hydrol Process* 23:2970–2980
- Weslien P, Klemetsson AK, Borjesson G et al (2009) Strong pH influence on N₂O and CH₄ fluxes from forested organic soils. *Eur J Soil Sci* 60:311–320
- Westman CJ (1995) A simple device for sampling of volumetric forest soil cores. *Silva Fennica* 29:247–251
- Yamulki S, Harrison RM, Goulding KWT et al (1997) N₂O, NO and NO₂ fluxes from a grassland: effect of soil pH. *Soil Biol Biochem* 29:1199–1208
- Yu KW, Faulkner SP, Baldwin MJ (2008) Effect of hydrological conditions on nitrous oxide, methane, and carbon dioxide dynamics in a bottomland hardwood forest and its implication for soil carbon sequestration. *Global Change Biol* 14:798–812